Following gluonic world lines to find the QCD coupling in the infrared

D. Antonov[a], H.-J. Pirner

Institut für Theoretische Physik, Universität Heidelberg, Philosophenweg 19, 69120 Heidelberg, Germany

Abstract. Using a parametrization of the Wilson loop with the minimal-area law, we calculate the polarization operator of a valence gluon, which propagates in the confining background. This enables us to obtain the infrared freezing (i.e. finiteness) of the running strong coupling in the confinement phase, as well as in the deconfinement phase up to the temperature of dimensional reduction. The momentum scale defining the onset of freezing is found both analytically and numerically. The nonperturbative contribution to the thrust variable, originating from the freezing, makes the value of this variable closer to the experimental one.

1 Introduction

The path-integral representation for the Green function of a particle moving along a closed trajectory and interacting with the gauge field yields the Wilson loop. When the particle is confined by the gauge field, its Wilson loop obeys the area law. In this physically very important case the path integral cannot be calculated analytically, because finding the minimal surface for an arbitrary contour $x_\mu(\tau)$ in $d > 2$ dimensions is too complicated. Therefore, effective parametrizations of the minimal surface have been invented in the literature (see e.g. [1–4]), which means that there exist certain physically motivated tricks to construct the minimal-area functional in terms of $x_\mu(\tau)$.

To give an example we consider the following formula, which converts a double surface integral into line integrals with Stokes' theorem:

$$\int_\Sigma \mathrm{d}\sigma_{\mu\nu}(x) \int_\Sigma \mathrm{d}\sigma_{\mu\rho}(x')\partial_\nu\partial_\rho D(x-x')$$
$$= -\oint_C \mathrm{d}x_\mu \oint_C \mathrm{d}x'_\mu D(x-x'). \qquad (1)$$

Here D is an arbitrary function for which the integrals are finite, $\partial_\nu \equiv \frac{\partial}{\partial x_\nu}$, and Σ is an arbitrary surface encircled by the contour C. As one can see, the choice $D(x-x') = (x-x')^2$ is the unique one, for which the derivatives on the L.H.S. of (1) are removed completely, and one obtains

$$\int_\Sigma \mathrm{d}\sigma_{\mu\nu}(x) \int_\Sigma \mathrm{d}\sigma_{\mu\nu}(x') = \oint_C \mathrm{d}x_\mu \oint_C \mathrm{d}x'_\mu x_\nu x'_\nu.$$

[a] e-mail: dima@tphys.uni-heidelberg.de

Now, if C is a flat contour, then we can choose Σ flat as well, in which case the L.H.S. of this equation equals $2S^2$, where S is the area of Σ. Therefore, for a flat contour, the minimal area reads

$$S = \sqrt{\frac{1}{2}\Sigma_{\mu\nu}^2}, \qquad (2)$$

where $\Sigma_{\mu\nu} \equiv \oint_C \mathrm{d}x_\mu x_\nu$ is the so-called tensor area [2–4], which is manifestly a functional of C only. Flat contours are a good approximation for particle trajectories when the particle is heavy. For example, the parametrization of (2) reproduces correctly the heavy-quark condensate [5, 6] and the mixed heavy-quark–gluon condensate [7] in QCD. However, it certainly cannot be correct for a light particle, whose trajectory may deviate significantly from the flat one.

A parametrization for light and even massless particles has been proposed in [8]. Similarly to (2), it allows one to express the area $S_{\min}$ of the minimal surface Σ in terms of a single integral. The main idea is to convert the proper time in the path integral to a length coordinate $\tau \in [0, R]$. After that, one can naturally parametrize $S_{\min}$ as an integral of the transverse direction, $|\mathbf{r}(\tau)|$, along this coordinate:

$$S_{\min} = \int_0^R \mathrm{d}\tau |\mathbf{r}(\tau)|. \qquad (3)$$

With such a parametrization of $S_{\min}$, we calculate in this paper the polarization operator of a gluon when it splits into two valence gluons. The latter move in a nonperturbative background, which confines them. In the absence of the confining background, the polarization operator yields the standard Yang–Mills one-loop running coupling [9]. In the presence of the background, the running

coupling goes to a constant in the infrared region, i.e. its logarithmic growth "freezes" [8]:

$$\alpha_{\mathrm{s}}(p) = \frac{4\pi}{b \ln \frac{p^2}{\Lambda^2}} \to \frac{4\pi}{\tilde{b} \ln \frac{p^2+m^2}{\Lambda^2}} \,. \qquad (4)$$

Here,

$$b = \frac{11}{3} N_c$$

is the absolute value of the first coefficient of the Yang–Mills β-function, and $m \propto$ (string tension)$^{1/2}$ is a nonperturbative mass parameter.

In this paper, we will show how freezing occurs and calculate the values of m and $\tilde{b}$ both analytically and numerically. The paper is organized as follows. In Sect. 2, we recall the derivation of $\alpha_{\mathrm{s}}(p)$ in the absence of the confining background, introducing the scalar polarization operator $\Pi_{\mathrm{free}}(p^2)$. In Sect. 3, the world-line integrals for the polarization operator $\Pi(x, y)$ in the coordinate representation are evaluated. In Sect. 4, freezing is discussed in detail. In Sect. 5, we extend this approach to the analysis of freezing in the deconfined phase. In Sect. 6, possible phenomenological consequences of freezing are discussed. Finally, the main results of the paper are summarized in the conclusions.

2 Polyakov's derivation of the running strong coupling

In this section, we recollect some steps of the derivation of $\alpha_{\mathrm{s}}(p)$ based on the integration over quantum fluctuations of the Yang–Mills field [9, 10]. The procedure starts with splitting the total Yang–Mills field A_μ^a into a background, $\bar{A}_\mu^a$, and a quantum fluctuation, a_μ^a, whose momentum is larger than that of the background. One can therefore substitute the Ansatz $A_\mu^a = \bar{A}_\mu^a + a_\mu^a$ into the bare Yang–Mills action,

$$S_0[A] = \frac{1}{4g_0^2} \int \mathrm{d}^4 x (F_{\mu\nu}^a[A])^2 \,,$$

where $F_{\mu\nu}^a[A]$ is the QCD field-strength tensor and g_0 is the bare coupling.

$$A_\mu^a = \bar{A}_\mu^a + a_\mu^a \,.$$

Fixing the so-called background Feynman gauge $(D_\mu a_\mu)^a = 0$, one adds to the action the term

$$S_{\mathrm{g.f.}} = \frac{1}{2g_0^2} \int \mathrm{d}^4 x \left[(D_\mu a_\mu)^a \right]^2 \,,$$

where $(D_\mu a_\nu)^a = \partial_\mu a_\nu^a + f^{abc} \bar{A}_\mu^b a_\nu^c$. The total gluon action reads

$$S_0 + S_{\mathrm{g.f.}} = \frac{1}{4g_0^2} \int \mathrm{d}^4 x \Big\{ \left(F_{\mu\nu}^a[\bar{A}] \right)^2 - 4 a_\nu^a \left(D_\mu F_{\mu\nu}[\bar{A}] \right)^a$$
$$- 2 a_\mu^a \left[\delta_{\mu\nu} (D^2)^{ac} + 2 f^{abc} F_{\mu\nu}^b[\bar{A}] \right] a_\nu^c + \mathcal{O}(a^3) \Big\} \,.$$

To perform the one-loop renormalization of g^2, one has to integrate out the a_μ^a-gluons in the $\bar{A}_\mu^a$-background. The full renormalized effective action can be written as

$$S = S_0 + S^{\mathrm{dia}} + S^{\mathrm{para}} = \int \frac{\mathrm{d}^4 p}{(2\pi)^4} \frac{1}{4g^2(p)} F_{\mu\nu}^a(p) F_{\mu\nu}^a(-p) \,, \qquad (5)$$

where the running coupling $g(p)$ is the object of the calculation. The so-called diamagnetic part of the effective action for $\bar{A}_\mu^a$-fields has the form

$$S^{\mathrm{dia}} = \mathrm{tr} \ln(-D^2) =$$
$$\mathrm{tr} \left[(-\partial^2)_{xx}^{-1} \Delta^{(2)}(x) - \frac{1}{2} (-\partial^2)_{xy}^{-1} \Delta^{(1)}(y) (-\partial^2)_{yx}^{-1} \Delta^{(1)}(x) \right] \,, \qquad (6)$$

where we have used the decomposition

$$-D^2 = -\partial^2 + \Delta^{(1)} + \Delta^{(2)} \,,$$
$$\Delta^{(1)}(x) \equiv \mathrm{i} t^a \left(\partial_\mu \bar{A}_\mu^a + 2 \bar{A}_\mu^a \partial_\mu \right) \,, \quad \Delta^{(2)}(x) \equiv (\bar{A}_\mu^a t^a)^2 \,,$$

$(t^a)^{bc} = -\mathrm{i} f^{abc}$. The paramagnetic part of the effective action reads

$$S^{\mathrm{para}} = \frac{1}{2} \mathrm{tr} \ln \left[1 + (-\partial^2)^{-1} (2 f^{abc} F_{\mu\nu}^b) \right]$$
$$= -\frac{1}{4} (-\partial^2)_{xy}^{-1} (2 f^{abc} F_{\mu\nu}^b(y)) (-\partial^2)_{yx}^{-1} (2 f^{adc} F_{\mu\nu}^d(x)) \,. \qquad (7)$$

The subscript "dia" describes the diamagnetic interaction of the $\bar{A}_\mu^a$-field with the orbital motion of the a_μ^a-gluons. This effect leads to the screening of charge and is present in the Abelian case as well. The subscript "para" is because this part of the effective action describes the paramagnetic interaction of the $\bar{A}_\mu^a$-field with the spin of the a_μ^a-gluons. It leads to the antiscreening of charge, which is a specific property of the non-Abelian gauge theories. The dia- and paramagnetic parts of the one-loop effective action can be written as

$$S \begin{Bmatrix} \mathrm{dia} \\ \mathrm{para} \end{Bmatrix} = N_c \begin{Bmatrix} \frac{1}{12} \\ (-1) \end{Bmatrix} \int \frac{\mathrm{d}^4 p}{(2\pi)^4} F_{\mu\nu}^a(p) F_{\mu\nu}^a(-p) \Pi_{\mathrm{free}}(p^2) \,, \qquad (8)$$

where

$$\Pi_{\mathrm{free}}(p^2) \equiv \frac{1}{16\pi^2} \ln \frac{\Lambda_0^2}{p^2} = \int \frac{\mathrm{d}^4 q}{(2\pi)^4} \frac{1}{q^2 (q+p)^2} \qquad (9)$$

is the free scalar polarization operator. Equation (5) then yields

$$\frac{1}{g^2(p)} = \frac{1}{g_0^2} - \frac{b}{16\pi^2} \ln \frac{\Lambda_0^2}{p^2} \,, \qquad (10)$$

where $g_0 \equiv g(\Lambda_0)$. Introducing the renormalized cutoff $\Lambda = \Lambda_0 \exp\left(-\frac{8\pi^2}{bg_0^2}\right)$, one finally arrives at the standard result $\alpha_{\mathrm{s}}(p) = \frac{4\pi}{b \ln \frac{p^2}{\Lambda^2}}$.

3 Calculation of the polarization operator

In reality, the gluon fluctuations a_μ^a do not appear as measurable excitations in the QCD spectrum and therefore must be self-confined, which means that the two a_μ^a-gluons propagating along the loop interact and form a colored bound state. This interaction has a one-gluon-exchange part plus a nonperturbative part, which may be related to string formation in the octet–octet channel coupled to a color octet. If one assumes Casimir scaling for the string tension, the corresponding string tension in the octet channel is related to that of the fundamental representation as (see e.g. [11]) $\sigma = \frac{9}{8}\sigma_{\text{fund}} = 0.225\,\text{GeV}^2$ with $\sigma_{\text{fund}} = 0.2\,\text{GeV}^2$. The a_μ^a-gluons may be confined because of a stochastic background field B_μ^a, whose momenta are even smaller than the momenta of the $\bar{A}_\mu^a$-gluons [8] (see Fig. 1). The presence of this additional background field can be taken into account by substituting into the Yang–Mills action a modified Ansatz

$$A_\mu^a = B_\mu^a + \bar{A}_\mu^a + a_\mu^a.$$

Accordingly, the definition of the one-loop effective action includes now the average over the background: $S = -\ln\left\langle \int \mathcal{D}a_\mu^a e^{-S[A]}\right\rangle_B$, where $\langle\dots\rangle_B$ is some gauge- and O(4)-invariant integration measure. In the course of the calculation of $\int \mathcal{D}a_\mu^a e^{-S[A]}$, the presence of the background leads to the substitution $\partial^2 \to D^2[B]$ in (6) and (7), where $(D_\mu[B]a_\nu)^a = \partial_\mu a_\nu^a + f^{abc}B_\mu^b a_\nu^c$. In the diagrammatic language, we are still considering the same one-loop diagrams, which contain *only two* external lines of the $\bar{A}_\mu^a$-field, *but* with the internal a_μ^a-loop receiving *infinitely many* contributions of the B_μ^a-field. The latter appear through the path-integral representation of the operator $(D^2[B])^{-1}$, which contains the Wilson line of the a_μ^a-gluon in the B_μ^a-field. Such an a_μ^a-gluon is called a valence gluon from now on.

In the coordinate representation the scalar polarization operator has the general form

$$\Pi_{\text{free}}(x) = \int \frac{\mathrm{d}^4 p}{(2\pi)^4} e^{\mathrm{i}px} \Pi_{\text{free}}(p^2) = D_0^2(x),$$
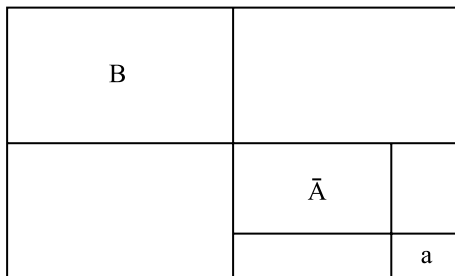$$D_0(x) = \frac{1}{4\pi^2 x^2}. \tag{11}$$

Fig. 1. Relative wavelengths of the three fields B_μ^a, $\bar{A}_\mu^a$, and a_μ^a

In an arbitrary background B_μ^a the polarization operator becomes

$$\langle \Pi(x,y|B)\rangle_B = \left\langle \text{tr}(D^2[B])_{xy}^{-1}(D^2[B])_{yx}^{-1}\right\rangle_B.$$

The path-integral representation of this average reads (see e.g. [8])

$$\langle \Pi(x,y|B)\rangle_B \equiv \Pi(x,y) = \int_0^\infty \mathrm{d}s \int_0^\infty \mathrm{d}\bar{s}$$
$$\times \int (\mathcal{D}z_\mu)_{xy}(\mathcal{D}\bar{z}_\mu)_{yx} \exp\left(-\int_0^s \mathrm{d}\lambda \frac{\dot{z}_\mu^2}{4} - \int_0^{\bar{s}} \mathrm{d}\bar{\lambda}\frac{\dot{\bar{z}}_\mu^2}{4}\right)$$
$$\times \left\langle \text{tr}\mathcal{P}\exp\left[\mathrm{i}\left(\int_0^s \mathrm{d}\lambda \dot{z}_\mu B_\mu^a(z)t^a + \int_0^{\bar{s}} \mathrm{d}\bar{\lambda}\dot{\bar{z}}_\mu B_\mu^a(\bar{z})t^a\right)\right]\right\rangle_B. \tag{12}$$

Here, $(\mathcal{D}z_\mu)_{xy}$ is the standard measure of integration over all paths $z_\mu(\lambda)$ such that $z(0) = y$ and $z(s) = x$. Namely, in d dimensions,

$$(\mathcal{D}z_\mu)_{xy} = \lim_{N\to\infty} \prod_{k=1}^N \int \frac{\mathrm{d}^d z_k}{(4\pi\varepsilon)^{d/2}},$$
$$z_k \equiv z(k\varepsilon), \quad \varepsilon = s/N.$$

The B_μ^a-averaged term in (12) is the Wilson loop of the valence gluon. The confinement of the latter is reflected in the so-called area law. The Wilson loop $\langle\dots\rangle_B$ can be approximated by $e^{-\sigma S_{\text{min}}}$, where $S_{\text{min}} = S_{\text{min}}[z,\bar{z}]$ is the area of the minimal surface encircled by the paths $z_\mu(s)$ and $\bar{z}_\mu(\bar{s})$. Moreover, parametrization of S_{min} in the form of (3) leads finally to the restoration of the translation invariance of $\Pi(x,y)$.

To calculate $\Pi(x,y)$ we introduce "center-of-mass" and relative coordinates of the gluons [8]:

$$u_\mu = \frac{\bar{s}z_\mu + s\bar{z}_\mu}{s + \bar{s}}, \quad r_\mu = z_\mu - \bar{z}_\mu.$$

We define new integration variables, which have the dimension of mass:

$$\mu = \frac{|x-y|}{2s}, \quad \bar{\mu} = \frac{|x-y|}{2\bar{s}}. \tag{13}$$

Then the kinetic terms of the gluons become

$$\int_0^s \frac{\dot{z}_\mu^2}{4}\mathrm{d}\lambda + \int_0^{\bar{s}} \frac{\dot{\bar{z}}_\mu^2}{4}\mathrm{d}\bar{\lambda} = \frac{1}{2}\int_0^R \mathrm{d}\tau \left[(\mu+\bar{\mu})\dot{u}_\mu^2 + \mu_r\dot{r}_\mu^2\right],$$

with

$$R \equiv |x-y|.$$

Here, $\mu_r \equiv \frac{\mu\bar{\mu}}{\mu+\bar{\mu}}$ is the "reduced mass", and τ is the distance to the point x along the line passing through x and y. Note that, unlike Schwinger's proper time s, which has the dimension (length)^2, the variable τ has the dimension (length). The minimal area, S_{min}, can be effectively parametrized with the coordinate τ alone, after which the

problem reduces to that of a Schrödinger equation with the potential $\sigma|\mathbf{r}|$. The main new idea of the present paper is to use a path-integral approach for the calculation of $\Pi(x,y)$. To this end, we will apply the Cauchy–Schwarz inequality to (3):

$$S_{\min} = \int_0^R d\tau |\mathbf{r}(\tau)| \leq \left(R \int_0^R d\tau \mathbf{r}^2 \right)^{1/2}. \qquad (14)$$

Note that, in case of a $(1+1)$-dimensional classical-mechanics problem, this approximation works with a good accuracy. For two particles of mass m interacting through a linear potential that move from $(y,t) = (0,0)$ to the point $(0,R)$, one can write the equation of motion $m\ddot{y}_1 = -m\ddot{y}_2 = -\sigma$. Substituting the solution, $y_1 = -y_2 = \frac{\sigma}{2m}t(R-t)$, into the exact formula $S_{\min} = \int_0^R dt(y_1 - y_2)$, we get $S_{\min} = \frac{\sigma R^3}{6m}$. Using instead our approximation, we obtain $S_{\min} \leq \left[R \int\limits_0^R dt(y_1 - y_2)^2 \right]^{1/2} = \frac{\sigma R^3}{\sqrt{30}m}$. The relative error is therefore quite small, namely $\left(\frac{1}{\sqrt{30}} - \frac{1}{6} \right) : \frac{1}{6} \simeq 0.096$.

Encouraged by this observation, we return to the $4d$ case and eliminate the square root in the Cauchy–Schwarz inequality, (14), by introducing an integration over an auxiliary parameter λ, which is sometimes called ein-bein. The expression for the polarization operator then becomes

$$\Pi(x,y) \simeq \frac{R^2}{4} \int_0^\infty \frac{d\mu}{\mu^2} \int_0^\infty \frac{d\bar{\mu}}{\bar{\mu}^2} \int (\mathcal{D}u_\mu)_{xy}(\mathcal{D}r_\mu)_{00}$$
$$\times \int_0^\infty \frac{d\lambda}{\sqrt{\pi\lambda}} \exp \left[-\lambda - \frac{\mu+\bar{\mu}}{2} \int_0^R d\tau \dot{u}_\mu^2 \right.$$
$$\left. - \frac{\mu_{\mathrm{r}}}{2} \int_0^R d\tau \dot{r}_\mu^2 - \frac{\sigma^2 R}{4\lambda} \int_0^R d\tau \mathbf{r}^2 \right]. \qquad (15)$$

Now, the integrals over $u_\mu(\tau)$ and $r_4(\tau)$ are free path integrals, while the integral over $\mathbf{r}(\tau)$ is that of a harmonic oscillator. We calculate these integrals by introducing the variables

$$\xi \equiv \sigma R^{3/2}/\sqrt{2\mu_{\mathrm{r}}\lambda} \quad \text{instead of } \lambda,$$
$$a = \mu R/2 \quad \text{instead of } \mu, \quad \text{and}$$
$$b = \bar{\mu} R/2 \quad \text{instead of } \bar{\mu}.$$

In terms of these variables

$$\Pi(x,y) \equiv \Pi(R) = \frac{\sigma}{16\pi^{9/2}R^2} f(\sigma R^2),$$

where

$$f(\sigma R^2) = \int_0^\infty \frac{d\xi}{\sqrt{\xi}\sinh^{3/2}\xi} \int_0^\infty da\,db\sqrt{\frac{a+b}{ab}}$$
$$\times \exp\left[-a-b-\left(\frac{\sigma R^2}{2\xi}\right)^2 \frac{a+b}{ab} \right]. \qquad (16)$$

When integrating analytically over a and b, it has been found (cf. Appendix A) that, owing to the $a \leftrightarrow b$ symmetry, the corresponding saddle-point equations can be solved even when the pre-exponent is lifted to the exponent. However, the leading *large-distance* asymptotic behavior of $\Pi(R)$ stems from the mere substitution of the saddle-point values without that lifting, $a = b \simeq \frac{\sigma R^2}{2\xi}$, into the pre-exponent (see Appendix A for details). This procedure yields

$$\Pi(R) \simeq \frac{\sigma^{3/2}}{16\pi^{7/2}R} \int_0^\infty \frac{d\xi}{\xi\sinh^{3/2}\xi} e^{-2\sigma R^2/\xi}. \qquad (17)$$

This integral can be evaluated by splitting the integration region into two parts:

$$\Pi(R) \equiv \frac{\sigma^{3/2}}{16\pi^{7/2}R}(I_1 + I_2), \qquad (18)$$

where

$$I_1 \simeq \int_0^1 \frac{d\xi}{\xi^{5/2}} e^{-2\sigma R^2/\xi}, \quad I_2 \simeq 2^{3/2} \int_1^\infty \frac{d\xi}{\xi} e^{-\frac{3\xi}{2} - \frac{2\sigma R^2}{\xi}}.$$

Then, at $\sigma R^2 \gg 1$, $I_1 = \mathcal{O}(e^{-2\sigma R^2})$ is a subleading term. The integral I_2 is saturated by its saddle point, $\xi = 2R\sqrt{\sigma/3}$, which lies inside the integration region. This yields

$$\Pi(R) \simeq \frac{\sigma^{5/4}}{2^{5/2}3^{1/4}\pi^3 R^{3/2}} e^{-2\sqrt{3\sigma}R} \quad \text{at} \quad \sigma R^2 \gg 1. \qquad (19)$$

Let us now consider the opposite limit of small distances. There, (A.3) goes over to $\left(\frac{\mu_{\mathrm{r}}}{2\pi R}\right)^{3/2}$, and the product of the three path integrals, (A.1)–(A.3), yields

$$\int (\mathcal{D}u_\mu)_{xy}(\mathcal{D}r_\mu)_{00}$$
$$\exp\left[-\frac{\mu+\bar{\mu}}{2} \int_0^R d\tau \dot{u}_\mu^2 - \frac{\mu_{\mathrm{r}}}{2} \int_0^R d\tau \dot{r}_\mu^2 - \frac{\sigma^2 R}{4\lambda} \int_0^R d\tau \mathbf{r}^2 \right]$$
$$\to \left[\frac{\mu\bar{\mu}}{(2\pi R)^2}\right]^2 \exp\left[-\frac{(\mu+\bar{\mu})R}{2} \right] \quad \text{at} \quad \sigma R^2 \ll 1.$$

Since this expression does not depend on λ anymore, the remaining λ-integration in (15) results in a factor of 1. Equation (15) then goes over to the free scalar polarization operator, (11):

$$\Pi(x,y) \to \frac{1}{64\pi^4 R^4} \int_0^\infty d\mu \int_0^\infty d\bar{\mu} \exp\left[-\frac{(\mu+\bar{\mu})R}{2} \right]$$
$$= \Pi_{\mathrm{free}}(x-y) \quad \text{at} \quad \sigma R^2 \ll 1. \qquad (20)$$

Therefore, we have a formula for the polarization operator, interpolating between the limits (19) and (20):

$$\Pi(R) = \frac{1}{16\pi^4 R^4} e^{-A\sqrt{\sigma R^2}} \left(1 + B(\sigma R^2)^{5/4} \right), \qquad (21)$$

with the following analytic values of the coefficients: $A = 2\sqrt{3} \simeq 3.46$ and $B = \frac{2^{3/2}\pi}{3^{1/4}} \simeq 6.75$.

4 Freezing of the running strong coupling at zero temperature

The integral of (16) has been also calculated with the Monte Carlo integration routine Vegas [12] in the interval $0.12 \leq \sigma R^2 \leq 4.3$. The interpolating curve is plotted in Fig. 2. The numerical fit to these data yields $A = 3.38$, which is very close to 3.46. The corresponding analytic and numerical values of the mass m in (4) are

$$m_{\mathrm{an}} = 2\sqrt{3\sigma} = 1.64\,\mathrm{GeV}\,, \quad m_{\mathrm{num}} = 3.38\sqrt{\sigma} = 1.60\,\mathrm{GeV}\,. \tag{22}$$

Note that the value of the analytically calculated freezing mass depends on the dimensionality of space-time d as

$$m_{\mathrm{an}} = 2\sqrt{(d-1)\sigma}\,. \tag{23}$$

This is readily seen from the saddle-point of the integral I_2 in (18) by noticing that, in d dimensions, $\sinh^{3/2}\xi \to \sinh^{\frac{d-1}{2}}\xi$ in (17). This result is a direct consequence of the Ansatz for the minimal area we use, (14).

Freezing, as defined by (4), stems from the replacement of the free-gluon polarization operator, (9), by that of the valence gluon,

$$\Pi_{\mathrm{val}}(p^2) \equiv \frac{1}{16\pi^2}\ln\frac{\Lambda_0^2}{p^2+m^2}\,. \tag{24}$$

Therefore, it looks instructive to compare the inverse Fourier image of this desired exact expression with our approximate result, (21). We have

$$\int \mathrm{d}^4 p\, e^{-ipx}\ln\frac{\Lambda_0^2}{p^2+m^2}$$
$$= \int_0^\infty \frac{\mathrm{d}s}{s}\int \mathrm{d}^4 p\, e^{-ipx}\left[e^{-s(p^2+m^2)} - e^{-s\Lambda_0^2}\right]$$
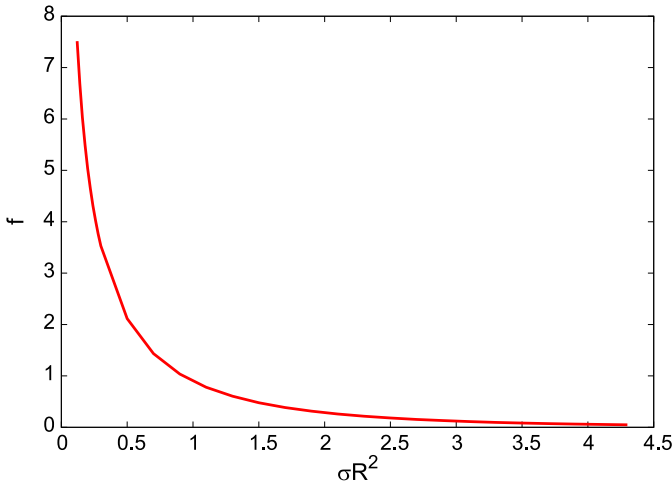$$= \pi^2 \int_0^\infty \frac{\mathrm{d}s}{s^3}e^{-\frac{x^2}{4s}-m^2 s} = \frac{8\pi^2 m^2}{x^2}K_2(m|x|)\,,$$

where K_2 is a Macdonald function. (When deriving the third formula in this chain, we have used the obvious fact that $\int \mathrm{d}^4 p\, e^{-ipx} = 0$ for $x \neq 0$.) Therefore, (24) in the coordinate representation reads

$$\Pi_{\mathrm{val}}(R) = \frac{m^2}{32\pi^4 R^2}K_2(mR)\,. \tag{25}$$

The short-distance asymptotic limit of this formula coincides with (20). As for the large-distance limit, we see that (25) has the same exponential fall-off as our result, (21), but a different pre-exponential R-behavior. The ratio of (21) to (25) at $mR \gtrsim 1$ is $\propto \sqrt{\sigma}R$. However, at large distances in question, this discrepancy is unimportant.

Finally, it is worthwhile to compare directly (24) with the Fourier image of (21). Because of the logarithmic divergency, we compare the derivatives of the two expressions, which are UV-finite. Therefore, we compare $\frac{\mathrm{d}\Pi_{\mathrm{val}}(p^2)}{\mathrm{d}p^2} = -\frac{1}{16\pi^2}\frac{1}{p^2+m^2}$ with $\frac{\mathrm{d}\Pi(p^2)}{\mathrm{d}p^2}$, where $\Pi(p^2)$ is the Fourier image of $\Pi(R)$: $\Pi(p^2) = \frac{4\pi^2}{|p|}\int_0^\infty \mathrm{d}R\,R^2 J_1(|p|R)\Pi(R)$, and the J_ν is the Bessel function. Introducing the dimensionless variables $x = \sqrt{\sigma}R$ and $q = |p|/\sqrt{\sigma}$, one has

$$\frac{\mathrm{d}\Pi(p^2)}{\mathrm{d}p^2} \equiv \frac{F(q)}{\sigma}\,,$$

where

$$F(q) = \frac{1}{8\pi^2 q^2}\int_0^\infty \frac{\mathrm{d}x}{x}\left[\frac{1}{2}\left(J_0(qx) - J_2(qx)\right) - \frac{J_1(qx)}{qx}\right]$$
$$\times \left(1 + Bx^{5/2}\right)e^{-Ax}\,. \tag{26}$$

This function has been calculated numerically for $0.02\,\mathrm{GeV} \leq |p| \leq 5\,\mathrm{GeV}$, which corresponds to $q \in [0.042, 10.541]$. Fitting the result by the function

$$F_{\mathrm{fit}}(q) = -\frac{1}{16\pi^2}\frac{d_1}{q^2+d_2^2}\,, \tag{27}$$

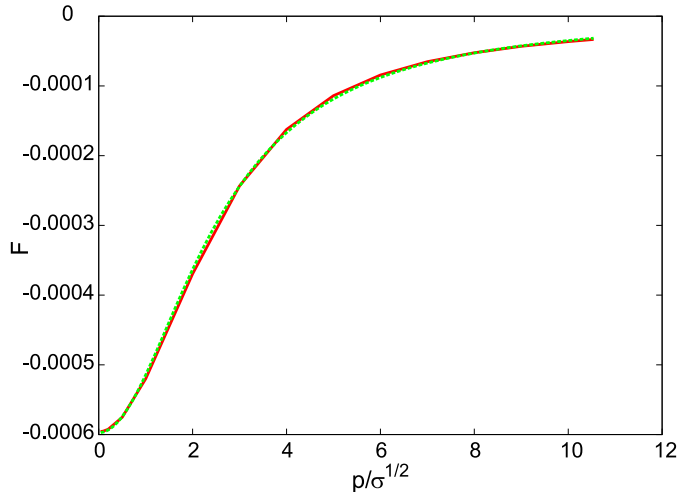**Fig. 2.** Integral $f(\sigma R^2)$ from (16)

Fig. 3. The function $F(q)$ (*red online*) and a fit to it (*green online*)

we obtain $d_1 = 0.585$ and $d_2 = 2.491$. The interpolating curve for $F(q)$, at the above-mentioned values of q, and the function (27) are plotted in Fig. 3. The value of m corresponding to the coefficient d_2 is therefore

$$m = d_2\sqrt{\sigma} = 1.18\,\text{GeV}\,. \tag{28}$$

It is closer to the phenomenological estimates ($\simeq 1\,\text{GeV}$) [13–15] than the values (22). Furthermore, the coefficient d_1 defines a numerical prediction for the parameter $\tilde{b}$:

$$\tilde{b} \simeq 0.585b = 6.435\,. \tag{29}$$

Therefore, the numerical analysis in the momentum representation yields an effective decrease of b in the infrared region. For the final form of $\alpha_s(p)$ at zero temperature, we refer the reader to the end of Sect. 5, where we discuss this result together with the one at $T > T_c$.

5 Freezing of the running strong coupling in the gluon plasma

At temperatures above deconfinement, $T > T_c$, large spatial Wilson loops still exhibit the area law. For pure gauge SU(3) Yang–Mills theory, $T_c \simeq 0.27\,\text{GeV}$ [16]. This behavior of spatial Wilson loops is the main well established nonperturbative phenomenon at $T > T_c$, which is usually called "magnetic" or "spatial" confinement [17–19]. Of course, it does not contradict true deconfinement of a static quark–antiquark pair, since space-time Wilson loops indeed lose the exponential damping with the area for $T > T_c$. If points x and y are separated by a time-like interval, valence gluons in the polarization operator $\Pi(x,y|T)$ are not confined, and therefore $\alpha_s(p^2)$ at $p^2 > 0$ is given by the perturbative formula, without freezing. When x and y are separated by a space-like interval, magnetic confinement holds, and one expects freezing of $\alpha_s(p^2)$ at $p^2 < 0$.

We will start our analysis with the calculation of the spatial polarization operator of a valence gluon in the SU(3) pure Yang–Mills theory at temperatures *higher* than the temperature of dimensional reduction, $T > T_{\text{d.r.}} \simeq 2T_c$. QCD becomes a superrenormalizable theory in three spatial dimensions, where the renormalization of the dimensionful coupling, $g_3 \equiv g\sqrt{T}$, is exact in one loop. Apparently, this effective coupling is not asymptotically free and is unrelated to the study of freezing. The following calculation prepares the subsequent analysis of α_s at $T_c < T < T_{\text{d.r.}}$.

Let us first consider the propagator of a free particle at temperature T from the origin to the point $R_\mu = (\mathbf{R}, R_4)$:

$$(-\partial^2)^{-1}_{R,0} = \int_0^\infty \mathrm{d}s \sum_n \frac{1}{(4\pi s)^2} \exp\left[-\frac{\mathbf{R}^2 + (R_4 - \beta n)^2}{4s}\right]$$
$$= \int_0^\infty \mathrm{d}s \sum_n \frac{1}{2T\sqrt{\pi s}} \exp\left[-\frac{(R_4 - \beta n)^2}{4s}\right]$$
$$\times T \int (\mathcal{D}\mathbf{z})_{\mathbf{R0}} \exp\left(-\int_0^s \frac{\dot{\mathbf{z}}^2}{4}\mathrm{d}\lambda\right)\,, \tag{30}$$

where $\sum_n \equiv \sum_{n=-\infty}^{+\infty}$. Upon performing Poisson resummation, one has

$$\frac{1}{2T\sqrt{\pi s}} \sum_n \exp\left[-\frac{(R_4 - \beta n)^2}{4s}\right] =$$
$$\sum_n \exp\left(-\omega_n^2 s + \mathrm{i}\omega_n R_4\right)\,, \quad \omega_n = 2\pi n T. \tag{31}$$

When $T \to \infty$, only the zeroth term on the R.H.S. of (31) survives, which means dimensional reduction. The sum goes to 1, and

$$(-\partial^2)^{-1}_{R,0} \to T \int_0^\infty \mathrm{d}s \int (\mathcal{D}\mathbf{z})_{\mathbf{R0}} \exp\left(-\int_0^s \frac{\dot{\mathbf{z}}^2}{4}\mathrm{d}\lambda\right)$$
$$= \frac{T}{4\pi L}\,, \tag{32}$$

where $L \equiv |\mathbf{R}|$. With the effect of magnetic confinement included, the polarization operator for $T > T_{\text{d.r.}}$ reads [cf. (12) and (14)]:

$$\Pi(\mathbf{x}, \mathbf{y}|T) = T^2 \int_0^\infty \mathrm{d}s \int_0^\infty \mathrm{d}\bar{s} I(s, \bar{s})\,,$$

where

$$I(s, \bar{s}) \simeq \int (\mathcal{D}\mathbf{z})_{\mathbf{xy}} (\mathcal{D}\bar{\mathbf{z}})_{\mathbf{yx}} \exp\left[-\int_0^s \frac{\dot{\mathbf{z}}^2}{4}\mathrm{d}\lambda - \int_0^{\bar{s}} \frac{\dot{\bar{\mathbf{z}}}^2}{4}\mathrm{d}\bar{\lambda}\right.$$
$$\left. - \sigma_s\left(L \int_0^L \mathrm{d}\tau \vec{\rho}^2\right)^{1/2}\right]. \tag{33}$$

Here, σ_s is the spatial string tension, whose ratio to the zero-temperature string tension, $\sigma_0 = 0.225\,\text{GeV}^2$, is plotted in Fig. 4. The points $\mathbf{x}$ and $\mathbf{y}$ are spatially separated, $\mathbf{y} - \mathbf{x} = \mathbf{R}$, and $\vec{\rho}$ is a two-dimensional vector orthogonal to $\mathbf{R}$. Two-dimensional vectors are denoted by an arrow, differently from three-dimensional vectors, which are boldfaced. This polarization operator can be calculated in a way similar to the zero-temperature one. Referring the reader for details to Appendix B, we present the final result: the polarization operator at $T > T_{\text{d.r.}}$ reads

$$\Pi(\mathbf{x}, \mathbf{y}|T) \simeq \frac{\sqrt{\sigma_s}T^2}{4\pi^2 L}\mathrm{e}^{-mL} \quad \text{at} \quad \sigma_s L^2 \gg 1, \tag{34}$$

$$\Pi(\mathbf{x}, \mathbf{y}|T) \simeq \left(\frac{T}{4\pi L}\right)^2 \quad \text{at} \quad \sigma_s L^2 \ll 1. \tag{35}$$

In (34),

$$m \equiv 2\sqrt{2\sigma_s}\,, \tag{36}$$

i.e. (23) at $d = 3$ is reproduced. Equation (35) is nothing but the free scalar polarization operator, which is just the square of (32).

Let us now proceed to the physically more interesting range of temperatures, $T_c < T < T_{\text{d.r.}}$. Here, like at $T = 0$, the exponential fall-off of $\Pi(x, y|T)$ (where x and y are four-vectors) due to magnetic confinement *is* relevant to
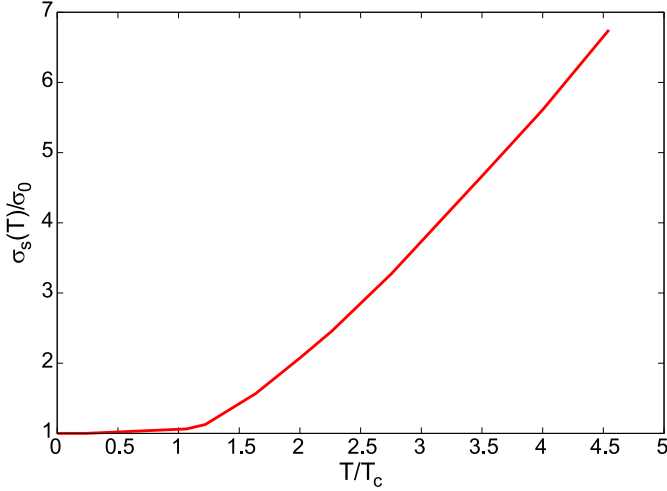
Fig. 4. The curve interpolating the lattice data on the ratio of the spatial string tension to the zero-temperature one in the SU(3) quenched QCD as a function of T/T_c [20, 21]

the freezing of α_s. The Euclidean path-integral representation for $\Pi(x, y|T)$ at $T_c < T < T_{d.r.}$ can be constructed by using (30) and (33):

$$\Pi(x, y|T) = \frac{1}{4\pi} \int_0^\infty \frac{ds}{\sqrt{s}} \int_0^\infty \frac{d\bar{s}}{\sqrt{\bar{s}}} I(s, \bar{s})$$
$$\times \sum_{n,k} \exp\left\{-\frac{1}{4}\left[\frac{(R_4 - \beta n)^2}{s} + \frac{(R_4 - \beta k)^2}{\bar{s}}\right]\right\}.$$
(37)

This quantity is calculated in Appendix B. At large distances, $\sigma_s L^2 \gg 1$, the result reads

$$\Pi(x, y|T) \simeq \frac{\sigma_s L}{8\sqrt{2}\pi^3 R^3} e^{-2\sqrt{2\sigma_s L R}},$$
(38)

where $R \equiv \sqrt{R_4^2 + L^2}$. Recalling that, in the physical Minkowski space-time, magnetic confinement holds only when R_μ is a space-like vector, one can always place the points x and y along some spatial axis, which makes L and R equal. The resulting formula for the polarization operator at large distances takes the form

$$\Pi(x, y|T) \simeq \frac{\sigma_s}{8\sqrt{2}\pi^3 R^2} e^{-2\sqrt{2\sigma_s} R} \quad \text{at} \quad \sigma_s R^2 \gg 1.$$
(39)

Therefore, at the temperatures $T_c < T < T_{d.r.}$ and Minkowskian $p^2 < 0$, freezing of $\alpha_s(p^2)$ takes place at the temperature-dependent momentum scale, which is analytically defined as $m = 2\sqrt{2\sigma_s}$. The factor "2" under the square root in this formula is the number of spatial dimensions minus one, in accordance with (23).

The limit of small distances is also discussed in Appendix B. At $L = R$, the result reads

$$\Pi(x, y|T) \to \left[\frac{T}{4\pi R} \coth(\pi T R)\right]^2 \quad \text{at} \quad \sigma_s R^2 \ll 1.$$
(40)

(In particular, at $T \to \infty$, this result goes over to (35), as it should.) Since $\sqrt{\sigma_0} = 474$ MeV and $T_c = 270$ MeV, one can see from Fig. 4 that, at $T_c < T < T_{d.r.}$, the condition $\sigma_s R^2 \ll 1$ automatically means also $TR \ll 1$. For this reason, at these temperatures, (40) can be approximated by its zero-temperature counterpart, $\frac{1}{(4\pi^2 R^2)^2}$. Therefore, the formula for the polarization operator, which interpolates between this short-distance limit and the large-distance one, (39), reads

$$\Pi(x, y|T) = \frac{e^{-2\sqrt{2\sigma_s} R}}{(4\pi^2 R^2)^2}\left(1 + \pi\sqrt{2}\sigma_s R^2\right)$$
$$\text{at} \quad T_c < T < T_{d.r.}.$$

Note that this expression depends on temperature only implicitly, namely through $\sigma_s(T)$.

The analysis of the polarization operator in the momentum representation can again be performed. Specifically, the factor $\left(1 + Bx^{5/2}\right)e^{-Ax}$ in (26) should be replaced by $\left(1 + \pi\sqrt{2}x^2\right)e^{-2\sqrt{2}x}$. Fitting the integral by the function (27), we get the values $d_1 = 0.711$ and $d_2 = 2.289$. The freezing mass grows with temperature as the square root of $\sigma_s(T)$: $m(T) = d_2\sqrt{\sigma_s(T)}$. When T varies from T_c to $T_{d.r.} \simeq 2T_c$, $m(T)$ varies from 1.09 GeV to 1.56 GeV. Finally, the parameter $\tilde{b} \simeq 0.711b = 7.821$ is larger than the one at zero-temperature, (29).

Both at $T = 0$ and $T_c < T < T_{d.r.}$, freezing modifies (10) to

$$\frac{1}{g^2(p)} = \frac{1}{g_0^2} - \frac{\tilde{b}}{16\pi^2} \ln\frac{\Lambda_0^2 + m^2}{p^2 + m^2}.$$

Defining the renormalized cutoff, Λ, through the bare one, Λ_0, by

$$\Lambda = \sqrt{\Lambda_0^2 + m^2} \exp\left(-\frac{2\pi}{\alpha_s(\Lambda_0)\tilde{b}}\right),$$

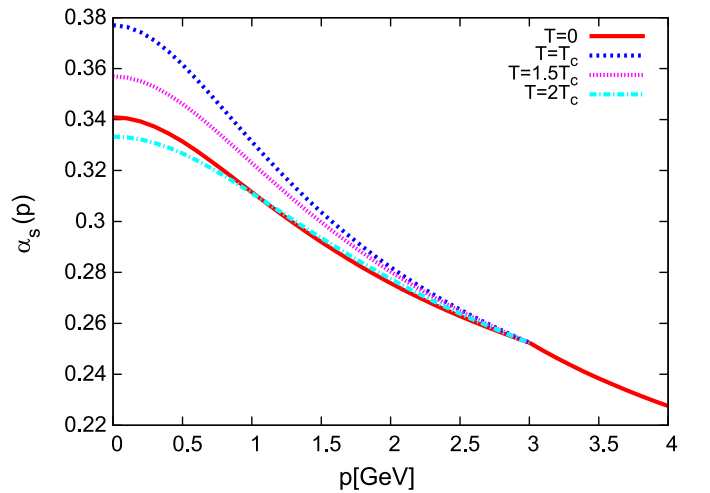**Fig. 5.** The running coupling with freezing at $0 \le p \le 3$ GeV for $T = 0$, $T = T_c$, $T = 1.5T_c$, and $T = 2T_c$. The curve at 3 GeV $\le p \le 4$ GeV is the experimental $\alpha_s(p)$, according to the web-site http://www-theory.lbl.gov/ ~ianh/alpha/alpha.html from [22]

one enforces $\alpha_{\mathrm{s}}(p) = \frac{4\pi}{\tilde{b}\ln\frac{p^2+m^2}{\Lambda^2}}$ to take the value $\alpha_{\mathrm{s}}(\Lambda_0)$ when $p = \Lambda_0$. It is then natural to choose a sufficiently large momentum scale Λ_0, where α_{s} is practically unaffected by freezing and finite-temperature effects, and match it at that scale to the experimental value. Choosing $\Lambda_0 = 3\,\mathrm{GeV}$, where $\alpha_{\mathrm{s}} \simeq 0.2524$, we plot in Fig. 5 $\alpha_{\mathrm{s}}(p)$ with freezing at $T = 0$, $T = T_{\mathrm{c}}$, $T = 1.5T_{\mathrm{c}}$, and $T = 2T_{\mathrm{c}}$ for $p \leq 3\,\mathrm{GeV}$, as well as the experimentally measured $\alpha_{\mathrm{s}}(p)$ [22] for $3\,\mathrm{GeV} \leq p \leq 4\,\mathrm{GeV}$. At fixed p, one observes an increase of $\alpha_{\mathrm{s}}(p)$ at $T = T_{\mathrm{c}}$ with respect to $\alpha_{\mathrm{s}}(p)$ at $T = 0$, and a subsequent decrease with the growth of T.

6 Possible phenomenological tests of the infrared freezing of the QCD coupling

It has been pointed out in various papers [23, 24] that the infrared behavior of the QCD running coupling can be used to estimate power-behaved corrections to various QCD observables. The essential parameters are a few moments of the coupling in the infrared region. One class of possible observables consists of event-shape variables like the thrust $\mathcal{T}$:

$$\mathcal{T} = \max_{\mathbf{n}} \frac{\sum_i |\mathbf{p}_i\mathbf{n}|}{\sum_i |\mathbf{p}_i|}\,.$$

Here the vectors $\mathbf{p}_i$ are the momenta of the final-state hadrons and $\mathbf{n}$ is an arbitrary vector that maximizes $\mathcal{T}$. If the momenta of the hadrons form an almost collinear jet then, after the maximization, $\mathbf{n}$ will lie along the jet axis. The value of the above thrust variable becomes 1 for an idealized pencil-like jet. Due to radiation of gluons, the observed $\mathcal{T}$ will be different from 1. In perturbative QCD, these corrections from hard-gluon radiation at a certain scale p can be calculated [25]. In addition to gluon radiation in the perturbative region, also soft-gluon radiation is present below a scale $\mu_{\mathrm{IR}} \simeq 3\,\mathrm{GeV}$. Essentially the physics in this region is supposed to be parametrized by the freezing of α_{s}, which we derived in this paper. Because of confinement, it seems to be impossible to map out this infrared running of the coupling exactly, i.e. for each momentum value. But measurements of the energy loss in fragmentation may allow one to access an integral over the infrared region. The observable $1 - \mathcal{T}$ related to thrust $\mathcal{T}$ has an expansion in terms of the perturbative $\alpha_{\mathrm{s}}^{\mathrm{pert}}(p)$:

$$1 - \mathcal{T}\Big|_{\mathrm{pert}} = 0.334\alpha_{\mathrm{s}}^{\mathrm{pert}}(p) + 1.02(\alpha_{\mathrm{s}}^{\mathrm{pert}}(p))^2 + \mathcal{O}\left((\alpha_{\mathrm{s}}^{\mathrm{pert}}(p))^3\right)\,,$$

which acquires a hadronization correction due to soft gluon radiation

$$1 - \mathcal{T} = 1 - \mathcal{T}|_{\mathrm{pert}} + \frac{2\lambda}{p}\,. \tag{41}$$

The nonperturbative higher-twist contribution λ may be related to an integral over the infrared region of $\alpha_{\mathrm{s}}(p) = $ $\frac{4\pi}{\tilde{b}\ln\frac{p^2+m^2}{\Lambda^2}}$ with freezing [24],

$$\lambda = C_F \int_0^{3\,\mathrm{GeV}} \mathrm{d}p \frac{\alpha_{\mathrm{s}}(p)}{\pi}\,,$$

where $C_F = 4/3$ is the Casimir operator of the fundamental representation of the group SU(3). Using for $\alpha_{\mathrm{s}}(p)$ the parameters m and $\tilde{b}$ at $T = 0$ and $T = T_{\mathrm{c}}$, we obtain

$$\lambda|_{T=0} = 0.376\,\mathrm{GeV}\,, \quad \lambda|_{T=0.27\,\mathrm{GeV}} = 0.395\,\mathrm{GeV}\,. \tag{42}$$

In order to reproduce the experimental data on the energy losses through radiation in the fragmentation process of c- and b-quarks, a value of $\lambda|_{T=0} = 0.5\,\mathrm{GeV}$ has been estimated [25].

As a possible phenomenological application of freezing, let us evaluate the thrust of a two-jet event at the scale $p = M_Z$. Using the value $\alpha_{\mathrm{s}}^{\mathrm{pert}}(M_Z) = 0.12$ [22], one obtains the purely perturbative contribution

$$1 - \mathcal{T}|_{\mathrm{pert}} = 0.334\alpha_{\mathrm{s}}^{\mathrm{pert}}(M_Z) + 1.02(\alpha_{\mathrm{s}}^{\mathrm{pert}}(M_Z))^2 \simeq 0.055\,, \tag{43}$$

which underestimates the experimental value measured at LEP [26], $1 - \mathcal{T} \simeq 0.068$. Inclusion of the higher-twist contribution according to (41), with the parameter λ given by (42), yields for the full quantity

$$1 - \mathcal{T}|_{T=0} = 0.063\,, \tag{44}$$

which is closer to the above-cited experimental value.

If hadronization takes place in the quark–gluon plasma, then one can study the effect of a modified $\alpha_{\mathrm{s}}(p)$ by investigating the energy loss due to soft radiation in the plasma. Accounting for the purely radiative higher-twist effect by means of $\lambda|_{T=0.27\,\mathrm{GeV}}$ from (42), one gets at the M_Z-scale

$$1 - \mathcal{T}|_{T=0.27\,\mathrm{GeV}} = 0.064\,. \tag{45}$$

If one instead uses $\alpha_{\mathrm{s}}(p)$ from [27, 28], then one gets $\lambda|_{T=0} = 1.03\,\mathrm{GeV}$ and $\lambda|_{T=0.27\,\mathrm{GeV}} = 0.61\,\mathrm{GeV}$, which overestimate the corresponding values (42), as well as the experimental value $\lambda|_{T=0} = 0.5\,\mathrm{GeV}$ [25].

In conclusion of this section, although $\alpha_{\mathrm{s}}(p)$ with freezing enhances the perturbative contribution (43) by 15%, the corresponding full values, (44) and (45), are still smaller than the experimental one. An increase of $\alpha_{\mathrm{s}}(p)$ at $T = T_{\mathrm{c}}$, with respect to the zero-temperature case, enhances the energy loss in the quark–gluon plasma, which occurs due to the infrared radiation. However, the amount of this enhancement, quantified by $(1 - \mathcal{T})$, is only 1.6%.

7 Conclusions

This paper analyzes the so-called IR freezing (i.e. finiteness) of the running strong coupling, in the confinement and deconfinement phases. The direct evaluation of the

path integral of a valence gluon confined by the stochastic background fields can be done by using the parametrization (14) for the minimal area. This parametrization reduces the path integral to that of the three-dimensional harmonic oscillator. In the deconfinement phase, at $T_c < T < T_{d.r.} \simeq 2T_c$, freezing of $\alpha_s(p)$ is present at Minkowskian $p^2 < 0$ due to the so-called magnetic confinement. Upon the calculation of the path integral, we find the momentum scales at which the freezing occurs in the confinement and deconfinement phases. Analytically, these scales are given by the same formula (23), where $d = 4$ at $T = 0$ and $d = 3$ at $T > T_c$ (cf. (36)). Numerically, the values of the freezing scales following from the fits in the momentum representation are smaller than the corresponding analytic ones and closer to the phenomenological value of 1 GeV (see (28) and the end of Sect. 5). The values of $\alpha_s(0)$ obtained at $T = 0$, T_c, $1.5T_c$, and $2T_c$ are 0.341, 0.377, 0.357, and 0.333, respectively. Full plots, which include the experimentally measured $\alpha_s(p)$, are presented in Fig. 5. Finally, we have estimated the physical effect of the freezing on the thrust variable. The calculated nonperturbative contribution, which arises due to the soft radiation, brings the purely perturbative value of this quantity closer to the experimental one.

Note in conclusion that one more application of the proposed method may be a calculation of the mean sizes of the gluon bound states. Such bound states can be not only color-singlet (glueball), but also color-octet (quark–gluon). The latter are suggested to be important ingredients of the quark–gluon plasma at temperatures $T_c < T < T_{d.r.}$ [11, 29–31].[1] Work in this direction is now in progress.

Note added in proof

When the present work was already in press, we have learned about the papers [33, 34], where nonperturbative contributions to the one-loop effective actions were also studied within the world-line formalism.

Appendix A: Details of calculation of $\Pi(x, y)$ at $T = 0$

The path integrals in (15) read as follows:

$$
\int (\mathcal{D}u_\mu)_{xy} \exp\left(-\frac{\mu + \bar{\mu}}{2} \int_0^R d\tau \dot{u}_\mu^2\right)
$$
$$
= \left(\frac{\mu + \bar{\mu}}{2\pi R}\right)^2 \exp\left[-\frac{(\mu + \bar{\mu})R}{2}\right], \qquad (A.1)
$$

[1] For a review see, e.g., [32].

$$
\int (\mathcal{D}r_4)_{00} \exp\left(-\frac{\mu_r}{2} \int_0^R d\tau \dot{r}_4^2\right) = \sqrt{\frac{\mu_r}{2\pi R}}, \qquad (A.2)
$$

$$
\int (\mathcal{D}\mathbf{r})_{00} \exp\left(-\frac{\mu_r}{2} \int_0^R d\tau \dot{\mathbf{r}}^2 - \frac{\sigma^2 R}{4\lambda} \int_0^R d\tau \mathbf{r}^2\right)
$$
$$
= \left[\frac{\omega}{4\pi \sinh\left(\frac{\omega R}{2\mu_r}\right)}\right]^{3/2}, \qquad (A.3)
$$

where $\omega \equiv \sigma\sqrt{2\mu_r R/\lambda}$ is the frequency of the harmonic oscillator. Bringing these formulae together and passing from the integration over λ to the integration over $\xi \equiv \sigma R^{3/2}/\sqrt{2\mu_r \lambda}$, we arrive at (16) as it would look like before the introduction of the variables a and b:

$$
\Pi(x, y) \simeq \frac{1}{2^{11/2}\pi^{9/2}} \frac{\sigma}{\sqrt{R}} \int_0^\infty \frac{d\xi}{\sqrt{\xi}\sinh^{3/2}\xi} \int_0^\infty \frac{d\mu\, d\bar{\mu}}{\sqrt{\mu_r}}
$$
$$
\times \exp\left[-\frac{\mu + \bar{\mu}}{2}R - \frac{\sigma^2 R^3}{2\xi^2}\left(\frac{1}{\mu} + \frac{1}{\bar{\mu}}\right)\right]. \qquad (A.4)
$$

It furthermore turns out that the saddle-point integral over μ and $\bar{\mu}$ can be done even with the account for $1/\sqrt{R\mu_r}$ in the pre-exponent. Indeed, we are dealing with the integral $\int_0^\infty d\mu\, d\bar{\mu} e^{-f(\mu,\bar{\mu})}$, where

$$
f(\mu, \bar{\mu}) \equiv \frac{\mu + \bar{\mu}}{2}R + \frac{\sigma^2 R^3}{2\xi^2}\left(\frac{1}{\mu} + \frac{1}{\bar{\mu}}\right) - \frac{1}{2}\ln\left[\frac{1}{R}\left(\frac{1}{\mu} + \frac{1}{\bar{\mu}}\right)\right].
$$

The saddle-point equation $\frac{\partial f}{\partial \bar{\mu}} = 0$ reads $R\bar{\mu}^2 + \mu_r - \frac{\sigma^2 R^3}{\xi^2} = 0$. We can further use the fact that, since f is symmetric under $\mu \leftrightarrow \bar{\mu}$, the saddle-point values of μ and $\bar{\mu}$ coincide. Therefore, setting in the last equation $\bar{\mu} = \mu$, we arrive at a quadratic equation, whose solution is

$$
\mu = \bar{\mu} = \frac{1}{4R}\left[-1 + \sqrt{1 + \left(\frac{4\sigma R^2}{\xi}\right)^2}\right]. \qquad (A.5)
$$

The sign "+" in front of the square root has been chosen because the integration region over μ and $\bar{\mu}$ is from 0 to $+\infty$.

Further, as we are interested in the large-distance regime, $\sigma R^2 \gtrsim 1$, we can consider separately the following three regions of integration over ξ:

- $\xi < 1 < 4\sigma R^2$. At these values of ξ, the saddle-point values (A.5) are $\mu = \bar{\mu} \simeq \frac{\sigma R}{\xi}$. Accordingly,

$$
e^{-f}\big|_{\text{saddle point}} = \frac{1}{R}\sqrt{\frac{2\xi}{\sigma}}e^{-2\sigma R^2/\xi}.
$$

Next, because f is a symmetric function of μ and $\bar{\mu}$, the pre-exponent of the saddle-point integral reads

$$
\frac{2\pi}{\frac{\partial^2 f}{\partial \bar{\mu}^2}\big|_{\text{saddle point}}} \simeq \frac{2\pi\sigma}{\xi}\left(1 + \frac{3}{8}\frac{\xi}{\sigma R^2}\right).
$$

Altogether,

$$\int_0^\infty \mathrm{d}\mu\,\mathrm{d}\bar\mu\,\mathrm{e}^{-f(\mu,\bar\mu)} \simeq \frac{2\pi}{R}\sqrt{\frac{2\sigma}{\xi}}\left(1+\frac{3}{8}\frac{\xi}{\sigma R^2}\right)\mathrm{e}^{-2\sigma R^2/\xi}\,. \tag{A.6}$$

Further, approximating $\frac{1}{\sqrt{\xi}\sinh^{3/2}\xi}$ in (A.4) by $\frac{1}{\xi^2}$ and changing the integration variable to $t=\frac{2\sigma R^2}{\xi}$, we have for the contribution to $\Pi(x,y)$ from this region of ξ's

$$\Pi^{(1)}(x,y) \simeq \frac{\sigma^{3/2}}{16\pi^{7/2}R}\left[\frac{1}{(2\sigma)^{3/2}R^3}\Gamma\left(\frac{3}{2},2\sigma R^2\right)\right.$$
$$\left.+\frac{3}{2^{7/2}\sigma^{3/2}R^3}\Gamma\left(\frac{1}{2},2\sigma R^2\right)\right],$$

where $\Gamma(\alpha,x)=\int_x^\infty \mathrm{d}t\,t^{\alpha-1}\mathrm{e}^{-t}$ is the incomplete Gamma-function. Using the known asymptotics $\Gamma(\alpha,x)\to x^{\alpha-1}\mathrm{e}^{-x}$ at $x>1$, we finally obtain

$$\Pi^{(1)}(x,y)\simeq\frac{\sigma^{1/2}\mathrm{e}^{-2\sigma R^2}}{32\pi^{7/2}R^3}\left(1+\frac{3}{8\sigma R^2}\right). \tag{A.7}$$

$- \ 1<\xi<4\sigma R^2$. In this region, (A.6) still holds, but $\frac{1}{\sqrt{\xi}\sinh^{3/2}\xi}$ in (A.4) should be approximated by $\frac{2^{3/2}}{\sqrt{\xi}\mathrm{e}^{3\xi/2}}$. This yields

$$\Pi^{(2)}(x,y)\simeq\frac{\sigma^{3/2}(I_1+I_2)}{(32\pi^7)^{1/2}R},$$
$$I_1\equiv\int_1^{4\sigma R^2}\frac{\mathrm{d}\xi}{\xi}\mathrm{e}^{-\frac{3\xi}{2}-\frac{2\sigma R^2}{\xi}},$$
$$I_2\equiv\frac{3}{8\sigma R^2}\int_1^{4\sigma R^2}\mathrm{d}\xi\,\mathrm{e}^{-\frac{3\xi}{2}-\frac{2\sigma R^2}{\xi}}. \tag{A.8}$$

Let us start with the analysis of I_1 by representing the integration region as $\int_1^{4\sigma R^2}=\int_0^\infty-\int_0^1-\int_{4\sigma R^2}^\infty$. Then the first of these three integrals can be done exactly and reads $2K_0(2\sqrt{3\sigma}R)$, where here and below the K_ν is a Macdonald function. We can further take into account that the saddle point of $\mathrm{e}^{-\frac{3\xi}{2}-\frac{2\sigma R^2}{\xi}}$, which is $\xi=2\sqrt{\sigma/3}R$, lies between 1 and $4\sigma R^2$. Owing to this fact, we can disregard $\frac{3\xi}{2}$ in the exponent of the integral $\int_0^1$, in the same way as we can disregard $\frac{2\sigma R^2}{\xi}$ in the exponent of the integral $\int_{4\sigma R^2}^\infty$. These approximations yield at $\sigma R^2>1$

$$I_1\simeq 2K_0(2\sqrt{3\sigma}R)-\Gamma(0,2\sigma R^2)-\Gamma(0,6\sigma R^2)$$
$$\to\sqrt{\frac{\pi}{\sqrt{3\sigma}R}}\mathrm{e}^{-2\sqrt{3\sigma}R}-\frac{\mathrm{e}^{-2\sigma R^2}}{2\sigma R^2}-\frac{\mathrm{e}^{-6\sigma R^2}}{6\sigma R^2}.$$

Analogously,

$$I_2\simeq\frac{3}{8\sigma R^2}\left[4R\sqrt{\frac{\sigma}{3}}K_1(2\sqrt{3\sigma}R)-\int_0^1\mathrm{d}\xi\,\mathrm{e}^{-2\sigma R^2/\xi}\right.$$
$$\left.-\int_{4\sigma R^2}^\infty\mathrm{d}\xi\,\mathrm{e}^{-3\xi/2}\right]\to\frac{3}{8\sigma R^2}$$
$$\times\left[2\sqrt{\frac{\pi R}{3}\sqrt{\frac{\sigma}{3}}}\mathrm{e}^{-2\sqrt{3\sigma}R}-\frac{\mathrm{e}^{-2\sigma R^2}}{2\sigma R^2}-\frac{2}{3}\frac{\mathrm{e}^{-6\sigma R^2}}{\sigma R^2}\right]$$
at $\ \ \sigma R^2>1\,.$

Equation (A.8) then yields

$$\Pi^{(2)}(x,y)\simeq\frac{\sigma^{3/2}}{(32\pi^7)^{1/2}R}\left[\frac{\pi^{1/2}}{(3\sigma)^{1/4}R^{1/2}}\left(1+\frac{1}{4R}\sqrt{\frac{3}{\sigma}}\right)\right.$$
$$\times\mathrm{e}^{-2\sqrt{3\sigma}R}-\frac{1}{2\sigma R^2}\left(1+\frac{3}{8\sigma R^2}\right)\mathrm{e}^{-2\sigma R^2}$$
$$\left.-\frac{5}{12}\frac{\mathrm{e}^{-6\sigma R^2}}{\sigma R^2}\right]. \tag{A.9}$$

$- \ 1<4\sigma R^2<\xi$. At these values of ξ, the saddle-point values of μ and $\bar\mu$, (A.5), can be approximated as $\mu=\bar\mu\simeq\frac{2\sigma^2R^3}{\xi^2}$. The exponent at the saddle point reads $\mathrm{e}^{-f}|_{\text{saddle point}}=\frac{\xi}{\sigma R^2}\mathrm{e}^{-\frac{1}{2}-\frac{2(\sigma R^2)^2}{\xi^2}}$. Again, owing to the symmetry of f under $\mu\leftrightarrow\bar\mu$, we find $\frac{\partial^2 f}{\partial\bar\mu^2}\Big|_{\text{saddle point}}\simeq\frac{\xi^4}{32\sigma^4R^6}$. Therefore, the saddle-point integral over μ and $\bar\mu$ reads

$$\int_0^\infty\mathrm{d}\mu\,\mathrm{d}\bar\mu\,\mathrm{e}^{-f(\mu,\bar\mu)}\simeq\frac{64\pi}{\sqrt{\mathrm{e}}}\frac{\sigma^3R^4}{\xi^3}\mathrm{e}^{-\frac{2(\sigma R^2)^2}{\xi^2}}\,.$$

Equation (A.4) then yields for the contribution to the polarization operator, which comes about from this region of ξ,

$$\Pi^{(3)}(x,y)\simeq\frac{4(\sigma R)^4}{\sqrt{\pi^7\mathrm{e}}}\int_{4\sigma R^2}^\infty\frac{\mathrm{d}\xi}{\xi^{7/2}}\mathrm{e}^{-\frac{3\xi}{2}-\frac{2(\sigma R^2)^2}{\xi^2}}\,.$$

The value of the saddle point of the exponent, $\xi=\frac{2(\sigma R^2)^{2/3}}{3^{1/3}}$, is smaller than $4\sigma R^2$, for which reason we approximately have

$$\Pi^{(3)}(x,y)\simeq\frac{4(\sigma R)^4}{\sqrt{\pi^7\mathrm{e}}}\int_{4\sigma R^2}^\infty\frac{\mathrm{d}\xi}{\xi^{7/2}}\mathrm{e}^{-\frac{3\xi}{2}}$$
$$=\sqrt{\frac{3^5}{2\pi^7\mathrm{e}}}(\sigma R)^4\Gamma\left(-\frac{5}{2},6\sigma R^2\right)$$
$$\simeq\frac{\sqrt{\sigma}}{48\sqrt{\pi^7\mathrm{e}}R^3}\mathrm{e}^{-6\sigma R^2}\,. \tag{A.10}$$

Bringing together (A.7), (A.9), and (A.10), we can write the final result for the polarization operator

$$\Pi(x, y) = \Pi^{(1)}(x, y) + \Pi^{(2)}(x, y) + \Pi^{(3)}(x, y):$$

$$\Pi(x, y) \simeq \frac{\sigma^{5/4}}{2^{5/2}3^{1/4}\pi^3 R^{3/2}} \left(1 + \frac{1}{4R}\sqrt{\frac{3}{\sigma}}\right) \mathrm{e}^{-2\sqrt{3\sigma}R}$$
$$+ \mathcal{O}\left(\mathrm{e}^{-2\sigma R^2}\right) + \mathcal{O}\left(\mathrm{e}^{-6\sigma R^2}\right),$$

where

$$\mathcal{O}\left(\mathrm{e}^{-2\sigma R^2}\right) \equiv \frac{1 - 2^{3/2}}{32\pi^{7/2}} \frac{\sigma^{1/2}}{R^3} \left(1 + \frac{3}{8\sigma R^2}\right) \mathrm{e}^{-2\sigma R^2},$$

$$\mathcal{O}\left(\mathrm{e}^{-6\sigma R^2}\right) \equiv \frac{\mathrm{e}^{-1/2} - 5 \cdot 2^{-1/2}}{48\pi^{7/2}} \frac{\sigma^{1/2}}{R^3} \mathrm{e}^{-6\sigma R^2}.$$

Note that the correction $\mathcal{O}\left(\mathrm{e}^{-6\sigma R^2}\right)$ is negative. The leading term, $\mathcal{O}\left(\mathrm{e}^{-2\sqrt{3\sigma}R}\right)$, comes about from (A.9).

Appendix B: Details of calculation of $\Pi(x, y)$ at $T > T_c$

Let us start with the polarization operator at $T > T_{\mathrm{d.r.}}$. Choosing for concreteness $\mathbf{R} = (L, 0, 0)$, we define the relative coordinate $\mathbf{r}(\tau) \equiv \mathbf{z}(\tau) - \bar{\mathbf{z}}(\tau) = (r_1(\tau), \vec{\rho}(\tau))$ and the "center-of-mass" coordinate $\mathbf{u} = \frac{\bar{s}\mathbf{z} + s\bar{\mathbf{z}}}{s + \bar{s}}$. After changing the variables $(s, \bar{s})$ to $(\mu, \bar{\mu})$ according to (13), we have for the polarization operator (33) [cf. (15)]

$$\Pi(\mathbf{x}, \mathbf{y}|T) \simeq \left(\frac{LT}{2}\right)^2 \int_0^\infty \frac{\mathrm{d}\mu}{\mu^2} \int_0^\infty \frac{\mathrm{d}\bar{\mu}}{\bar{\mu}^2} I(\mu, \bar{\mu}),$$
(B.1)

where

$$I(\mu, \bar{\mu}) = \int (\mathcal{D}\mathbf{u})_{\mathbf{xy}} (\mathcal{D}\mathbf{r})_{00} \int_0^\infty \frac{\mathrm{d}\lambda}{\sqrt{\pi\lambda}}$$
$$\times \exp\left[-\lambda - \frac{\mu + \bar{\mu}}{2}\int_0^L \mathrm{d}\tau \dot{\mathbf{u}}^2 - \frac{\mu_{\mathrm{r}}}{2}\int_0^L \mathrm{d}\tau \dot{\mathbf{r}}^2\right.$$
$$\left. - \frac{\sigma_{\mathrm{s}}^2 L}{4\lambda}\int_0^L \mathrm{d}\tau \vec{\rho}^2\right].$$

Carrying out the path integrations over $\mathbf{r}$ and $\mathbf{u}$, we have

$$I(\mu, \bar{\mu}) = \frac{\sigma_{\mathrm{s}} \mu \bar{\mu} \sqrt{\mu + \bar{\mu}}}{8\sqrt{2}\pi^{7/2} L^{3/2}} \exp\left[-\frac{(\mu + \bar{\mu})L}{2}\right]$$
$$\times \int_0^\infty \frac{\mathrm{d}\lambda}{\lambda} \frac{\mathrm{e}^{-\lambda}}{\sinh\left(\sigma_{\mathrm{s}}\sqrt{\frac{L^3}{2\mu_{\mathrm{r}}\lambda}}\right)}.$$
(B.2)

Changing the integration variable $\lambda \to \xi = \sigma_{\mathrm{s}}\sqrt{\frac{L^3}{2\mu_{\mathrm{r}}\lambda}}$, one can rewrite this equation as

$$I(\mu, \bar{\mu}) = \frac{\sigma_{\mathrm{s}}}{4\sqrt{2\pi^7 L^3}} \mu \bar{\mu} \sqrt{\mu + \bar{\mu}} \int_0^\infty \frac{\mathrm{d}\xi}{\xi \sinh \xi}$$
$$\times \exp\left\{-\frac{L}{2}\left[\mu + \bar{\mu} + \left(\frac{\sigma_{\mathrm{s}}L}{\xi}\right)^2\left(\frac{1}{\mu} + \frac{1}{\bar{\mu}}\right)\right]\right\}.$$
(B.3)

One should now substitute this expression into (B.1) and perform approximate saddle-point integrations over μ and $\bar{\mu}$. This procedure means the insertion of the saddle-point values into the pre-exponent. In this way, one arrives at the following counterpart of (17) at $T > T_{\mathrm{d.r.}}$:

$$\Pi(\mathbf{x}, \mathbf{y}|T) \simeq \frac{\sqrt{\sigma_{\mathrm{s}}}T^2}{8\pi^{5/2}L} \int_0^\infty \frac{\mathrm{d}\xi}{\sqrt{\xi}\sinh\xi} \mathrm{e}^{-2\sigma_{\mathrm{s}}L^2/\xi}.$$
(B.4)

Note that, in three dimensions, $\sinh^{\frac{d-1}{2}}\xi = \sinh\xi$, as explained after (23). By splitting the integration region as in (18), the last integral can be approximated as $I_1 + I_2$, where

$$I_1 \equiv \int_0^1 \frac{\mathrm{d}\xi}{\xi^{3/2}} \mathrm{e}^{-2\sigma_{\mathrm{s}}L^2/\xi}, \quad I_2 \equiv 2\int_1^\infty \frac{\mathrm{d}\xi}{\sqrt{\xi}} \mathrm{e}^{-\xi - 2\sigma_{\mathrm{s}}L^2/\xi}.$$

To evaluate these integrals notice that, at temperatures $T > T_{\mathrm{d.r.}}$, which we are currently considering, the spatial string tension is parametrically $\sigma_{\mathrm{s}} \propto g_3^2 \sim T^2$. Numerically, the ratio $\sigma_{\mathrm{s}}/\sigma_0$ is larger than 2 at $T > T_{\mathrm{d.r.}}$ (cf. Fig. 4). Next, for magnetic confinement to hold, the spatial Wilson loop should be sufficiently large, in particular the distance L should be $\gtrsim 1$ fm. For such distances, $2\sigma_{\mathrm{s}}L^2 > 4\sigma_0 L^2 \gg 1$, and we have

$$I_1 \simeq \frac{\mathrm{e}^{-2\sigma_{\mathrm{s}}L^2}}{2\sigma_{\mathrm{s}}L^2}, \quad I_2 \simeq 2\sqrt{\pi}\mathrm{e}^{-2\sqrt{2\sigma_{\mathrm{s}}}L} - \frac{\mathrm{e}^{-2\sigma_{\mathrm{s}}L^2}}{\sigma_{\mathrm{s}}L^2}.$$

Bringing these expressions together and neglecting the subleading terms $\sim \frac{\mathrm{e}^{-(mL/2)^2}}{(mL)^2}$, we arrive at (34).

In the opposite limit of small distances, (B.2) yields

$$I(\mu, \bar{\mu}) \to \frac{(\mu\bar{\mu})^{3/2}}{(2\pi L)^3} \exp\left[-\frac{(\mu + \bar{\mu})L}{2}\right].$$
(B.5)

Inserting this expression into (B.1), we have

$$\Pi(\mathbf{x}, \mathbf{y}|T) \to \frac{T^2}{32\pi^3 L} \int_0^\infty \frac{\mathrm{d}\mu}{\sqrt{\mu}} \int_0^\infty \frac{\mathrm{d}\bar{\mu}}{\sqrt{\bar{\mu}}} \exp\left[-\frac{(\mu + \bar{\mu})L}{2}\right]$$
$$\text{at} \quad \sigma_{\mathrm{s}}L^2 \ll 1.$$

Straightforward integrations over μ and $\bar{\mu}$ in this formula lead to (35).

Let us now consider the temperature interval $T_c < T < T_{\mathrm{d.r.}}$. Changing in (37) the variables $(s, \bar{s})$ to $(\mu, \bar{\mu})$, we have

$$\Pi(\mathbf{x}, \mathbf{y}|T) = \frac{L}{8\pi} \int_0^\infty \frac{\mathrm{d}\mu}{\mu^{3/2}} \int_0^\infty \frac{\mathrm{d}\bar{\mu}}{\bar{\mu}^{3/2}} I(\mu, \bar{\mu})$$
$$\times \sum_{n,k} \exp\left\{-\frac{1}{2L}\left[\mu(R_4 - \beta n)^2 + \bar{\mu}(R_4 - \beta k)^2\right]\right\}.$$
(B.6)

Using for $I(\mu, \bar{\mu})$ the representation (B.3) and performing the saddle-point integrations over μ and $\bar{\mu}$ as above, we ar-

rive at the following analogue of (B.4):

$$\Pi(x,y|T) \simeq \frac{\sigma_{\rm s}^{3/2}}{16\pi^3\sqrt{2\pi}L} \int_0^\infty \frac{{\rm d}\xi}{\xi^{3/2}\sinh\xi}$$
$$\times \sum_{n,k} \sqrt{\frac{\varphi_n+\varphi_k}{(\varphi_n\varphi_k)^3}}\, {\rm e}^{-\frac{\sigma_{\rm s}L^2}{\xi}(\varphi_n+\varphi_k)},$$

where

$$\varphi_n \equiv \sqrt{1+\left(\frac{R_4-\beta n}{L}\right)^2}.$$

When splitting the ξ-integral as in (18),

$$\int_0^\infty \frac{{\rm d}\xi}{\xi^{3/2}\sinh\xi}{\rm e}^{-\frac{\sigma_{\rm s}L^2}{\xi}(\varphi_n+\varphi_k)} \simeq$$
$$\int_0^1 \frac{{\rm d}\xi}{\xi^{5/2}}{\rm e}^{-\frac{\sigma_{\rm s}L^2}{\xi}(\varphi_n+\varphi_k)} + 2\int_1^\infty \frac{{\rm d}\xi}{\xi^{3/2}}{\rm e}^{-\xi-\frac{\sigma_{\rm s}L^2}{\xi}(\varphi_n+\varphi_k)},$$
$$\tag{B.7}$$

we notice that, at temperatures $T_{\rm c} < T < T_{\rm d.r.}$ of interest, the ratio $\sigma_{\rm s}/\sigma_0$ ranges between 1 and 2 (see Fig. 4). Therefore,

$$\sigma_{\rm s}L^2(\varphi_n+\varphi_k) \geq 2\sigma_{\rm s}L^2 > 2\sigma_0 L^2 \gg 1 \quad \text{at} \quad L \gtrsim 1\,{\rm fm}.$$

For this reason, the second of the two integrals on the R.H.S. of (B.7) is again saturated by its saddle point, $\xi_{\rm s.p.} = \sqrt{\sigma_{\rm s}L^2(\varphi_n+\varphi_k)}$, and yields the leading exponential fall-off with L, whereas the first integral yields a subleading Gaussian term. Disregarding the latter, we have for the leading exponential fall-off:

$$\Pi(x,y|T) \simeq \frac{\sigma_{\rm s}}{8\sqrt{2}\pi^3 L^2} \sum_{n,k} \frac{{\rm e}^{-2\sqrt{\sigma_{\rm s}L^2(\varphi_n+\varphi_k)}}}{(\varphi_n\varphi_k)^{3/2}}.$$

Now, as we have just seen, the argument of the exponent here is much larger than 1. Therefore, one can safely restrict oneself to the φ_0-terms in the sums over n and k. Since $\varphi_0 = R/L$, where $R \equiv \sqrt{R_4^2+L^2}$, we arrive at (38).

In the opposite case of small distances, inserting (B.5) into (B.6), we have

$$\Pi(x,y|T) \to \frac{1}{64\pi^4 L^2} \sum_{n,k} \int_0^\infty {\rm d}\mu \int_0^\infty {\rm d}\bar\mu$$
$$\times \exp\left[-\frac{L}{2}\left(\mu\varphi_n^2+\bar\mu\varphi_k^2\right)\right]$$
$$= \frac{1}{16\pi^4} \sum_{n,k} \frac{1}{\left[L^2+(R_4-\beta n)^2\right]\left[L^2+(R_4-\beta k)^2\right]}$$
$$\text{at} \quad \sigma_{\rm s}R^2 \ll 1. \tag{B.8}$$

Therefore, we have recovered in the short-distance limit the product of two free scalar thermal propagators. Note that the sums in (B.8) can be done analytically. Setting $L = R$ and $R_4 = 0$, we obtain (40).

References

1. A.Y. Dubin, A.B. Kaidalov, Y.A. Simonov, Phys. Lett. B **323**, 41 (1994)
2. A.M. Polyakov, Nucl. Phys. B **164**, 171 (1980)
3. M.A. Shifman, Nucl. Phys. B **173**, 13 (1980)
4. A.A. Migdal, Int. J. Mod. Phys. A **9**, 1197 (1994)
5. D. Antonov, JHEP **10**, 030 (2003)
6. D. Antonov, Nucl. Phys. B Proc. Suppl. **152**, 144 (2006)
7. D. Antonov, JHEP **10**, 018 (2005)
8. Y.A. Simonov, Phys. Atom. Nucl. **58**, 107 (1995)
9. A.M. Polyakov, Gauge Fields and Strings (Harwood Academic Publishers, Chur, 1987)
10. M.E. Peskin, D.V. Schroeder, An Introduction to Quantum Field Theory (Perseus Books Publishing, Reading, Massachusetts, 1995)
11. E.V. Shuryak, I. Zahed, Phys. Rev. D **70**, 054507 (2004)
12. G.P. Lepage, VEGAS: An Adaptive Multi-dimensional Integration Program, preprint CLNS-80/447, Cornell University, 1980
13. A.M. Badalian, A.I. Veselov, B.L.G. Bakker, Phys. Rev. D **70**, 016007 (2004)
14. D. Ebert, R.N. Faustov, V.O. Galkin, Phys. Rev. D **72**, 034026 (2005)
15. D. Ebert, R.N. Faustov, V.O. Galkin, Eur. Phys. J. C **47**, 745 (2006)
16. P. Petreczky, Eur. Phys. J. C **43**, 51 (2005)
17. Y.A. Simonov, JETP Lett. **54**, 249 (1991)
18. C. Borgs, Nucl. Phys. B **261**, 455 (1985)
19. E. Manousakis, J. Polonyi, Phys. Rev. Lett. **58**, 847 (1987)
20. G. Boyd, J. Engels, F. Karsch, E. Laermann, C. Legeland, M. Lütgemeier, B. Petersson, Nucl. Phys. B **469**, 419 (1996)
21. N.O. Agasian, Phys. Lett. B **562**, 257 (2003)
22. Particle Data Group, W.-M. Yao et al., J. Phys. G **33**, 1 (2006) (http://pdg.lbl.gov)
23. Y.L. Dokshitzer, G. Marchesini, B.R. Webber, Nucl. Phys. B **469**, 93 (1996)
24. Y.L. Dokshitzer, V.A. Khoze, S.I. Troian, Phys. Rev. D **53**, 89 (1996)
25. R.K. Ellis, W.J. Stirling, B.R. Webber, QCD and Collider Physics (Cambridge Univ. Press, Cambridge, 1996) Chapt. 5.6
26. Z. Kunszt, P. Nason, G. Marchesini, B.R. Webber, QCD at LEP, preprint ETH-PT-89-39 (in: Proc. 1989 LEP Physics Workshop, **1**, p. 373)
27. J. Braun, H. Gies, JHEP **06**, 024 (2006)
28. J. Braun, H.J. Pirner, Phys. Rev. D **75**, 054031 (2007)
29. S. Datta, F. Karsch, P. Petreczky, I. Wetzorke, Nucl. Phys. Proc. Suppl. **119**, 487 (2003)
30. S. Datta, F. Karsch, P. Petreczky, I. Wetzorke, Phys. Rev. D **69**, 094507 (2004)
31. M. Asakawa, T. Hatsuda, Phys. Rev. Lett. **92**, 012001 (2004)
32. N. Brambilla et al., preprint hep-ph/0412158, Chapt. 7
33. S.J. Huber, A. Laser, M. Reuter, M.G. Schmidt, Nucl. Phys. B **539**, 477 (1999)
34. S.J. Huber, M. Reuter, M.G. Schmidt, Phys. Lett. B **462**, 158 (1999)